

The effect of tangled magnetic fields on instabilities in tokamak plasmas

A.J. Thornton¹, A. Kirk¹, J.R. Harrison¹, P. Cahyna², I.T. Chapman¹, E. Nardon³ and the MAST team

¹ EURATOM/CCFE Fusion Association, Culham Science Centre, Abingdon, Oxon, OX14 3DB, UK

² Institute of Plasma Physics AS CR v.v.i., Association EURATOM/IPP.CR, Prague, Czech Republic

³ Association Euratom/CEA, CEA Cadarache, F-13108, St. Paul-lez-Durance, France

E-mail: andrew.thornton@ccfe.ac.uk

Abstract. The high pressure gradients in the edge of a tokamak plasma can lead to the formation of explosive plasma instabilities known as edge localised modes (ELMs). The control of ELMs is an important requirement for the next generation of fusion devices such as ITER. Experiments performed on the Mega Amp Spherical Tokamak (MAST) at Culham have shown that the application of non-axisymmetric resonant magnetic perturbations (RMPs) can be used to mitigate ELMs. During the application of the RMPs, clear structures are observed in visible-light imaging of the X-point region. These lobes, or tangles, have been observed for the first time and their appearance is correlated with the mitigation of ELMs. Tangle formation is seen to be associated with the RMPs penetrating the plasma and may be important in explaining why the ELM frequency increases during ELM mitigation. Whilst the number and location of the tangles can be explained by vacuum magnetic field modelling, obtaining the correct radial extent of the tangles requires the plasma response to be taken into account.

1. Introduction

In tokamaks, when sufficient external heating power is applied, there is a transition between a low confinement mode (L mode) and a high confinement mode (H mode) (Wagner *et al.* (1982)). The H mode plasma is characterised by decreased cross field transport and steep gradients in both current and pressure at the plasma edge. The build up of pressure at the plasma edge continues until a stability limit is reached, at which point the pressure at the edge of the plasma collapses as shown in Figure 1 and a filament of plasma is ejected. The instability which results in the ejection of a filament of plasma is known as an edge localised mode (ELM) (Zohm (1996)). An example of an ELM from the Mega Amp Spherical Tokamak (MAST) is shown in Figure 2 and was captured using high speed visible imaging of the plasma. The typical duration of an ELM in MAST is 200 μ s, with a single ELM carrying between 5% and 20% of the energy at the edge of the plasma (Kirk *et al.* (2004)). Following an ELM, the current and pressure profiles recover and the pressure begins to increase at the edge once more, the cycle then repeats itself thorough the duration of the discharge.

The energy carried by the ELM can give rise to significant heat fluxes to the exhaust system of the tokamak, known as the divertor. The high heat fluxes are a concern for the next generation



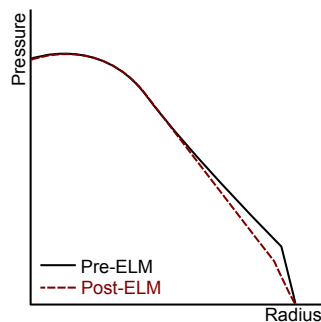


Figure 1. A schematic diagram showing the pressure before (black solid line) and the pressure after (red dashed line) an ELM event. The ELM carries away the energy at the edge of the plasma.

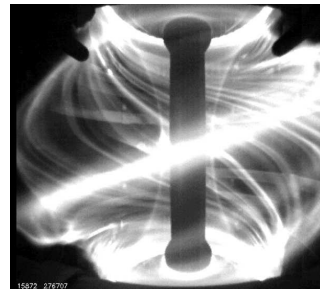


Figure 2. Visible emission from an ELM emitted during a MAST discharge. The filament is ejected out of the plasma and is aligned to the magnetic field.

of fusion devices, such as ITER where the energy released from an ELM is expected to be 20 MJ in $500 \mu\text{s}$ (Loarte *et al.* (2007)) producing a heat flux on the divertor surfaces of 20 MJ m^{-2} . The high heat loads generated by ELMs would limit the lifetime of the ITER divertor, resulting in the replacement of the divertor being necessary. It is clear that a means of ELM control is required to mitigate the heat loads to the divertor in future devices.

One scheme of ELM mitigation is the use of 3D magnetic perturbations to modify the nested 2D flux surfaces at the edge of the plasma. The modification of the flux surface is achieved using a non-axisymmetric perturbation which is applied using coils, known as a resonant magnetic perturbation (RMP) (Evans *et al.* (2004)). These RMP fields are a radial field at the plasma edge which is thought to generate magnetic islands. When the overlap of adjacent island chains forms a stochastic or ergodic region, this prevents the build up of pressure and leads to ELM mitigation.

In order to fully understand the effect of mitigation via RMP, the plasma response to the 3D field must be understood. The plasma response is the screening out of the external RMP field by the plasma which affects the penetration of the field into the plasma and the formation of the magnetic islands. The application of the RMP affect the frequency at which the ELMs occur and as such lead to a change in the stability of the plasma. The effect of the RMP on the stability of the plasma is another key area of research for RMP physics, along with the plasma response. In the case of ELM control, the reduction in the pressure profile could be a result of increased cross field transport, however, this would lead to reduction of the ELM frequency which is not always seen experimentally. This work aims to study the plasma response to the applied field and determine the implications the RMP have on plasma stability.

2. Mitigation of edge localised modes (ELMs)

ELM control via RMP can take two forms, firstly the technique can lead to the elimination of the ELMs from the discharge which is known as ELM suppression and has been achieved on DIII-D (Evans *et al.* (2004)). Alternatively, RMP field could lead to an increase in the ELM frequency with a corresponding decrease in the ELM size, which is known as ELM mitigation. The product of the ELM frequency and the ELM size has been found to be constant. The peak heat flux to the divertor surfaces, which is the source of the damage, scales with the ELM size, therefore a decrease in the ELM size decreases the effect on the divertor (Federici *et al.* (2003)).

MAST is fitted with 18 RMP coils for ELM mitigation studies, 12 coils are located below the midplane of the device, equally spaced around the circumference of the plasma, with the remaining 6 equally spaced above the midplane (Kirk *et al.* (2013)). Figure 3 shows the effect of applying the RMP coils on an ELMing MAST discharge. The D_α emission from the plasma in the coils off case is shown in the middle panel in Figure 3. The ELMs are the sudden increases in the D_α light and are generated by the ejected filament striking the neutral gas surrounding the plasma, causing it to emit. The H mode period starts at 0.24s and the first ELM occurs at 0.26s. The RMP coil current is shown in the top panel of Figure 3 and the effect on the ELMs in the bottom panel. It is clear that the ELM frequency increases during the coils on period and the amplitude of the D_α emission decreases showing that the ELM size also falls. When the coils are turned off the ELM size and frequency return to that seen in the coils off case.

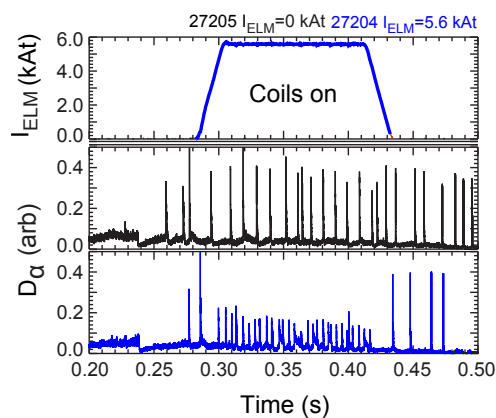


Figure 3. The effect of the application of the RMP coils is shown in these two discharges. The coil current in the coils is shown in the top panel. The centre and bottom panel shows the D_α light emitted from the plasma as a function of time for two shots, one without the coils on (centre panel) and one with the coils on (bottom panel).

3. Effect of 3D fields on tokamak equilibria

The magnetic field is toroidally symmetric prior to the application of the RMP coils, however, the RMP coils cause the toroidal symmetry to be lost and the field becomes three dimensional. The 3D field causes the field lines to behave as a trajectory on a Hamiltonian system when the coils are applied (Evans *et al.* (2005)). The effect of this can be seen in Figure 4 which shows the plasma boundary, known as the last closed flux surface (LCFS) or separatrix for a plasma with the coils off (panel (a)) and for the coils on (panel (b)). In the coils off case, if a field line on the LCFS is followed around the tokamak in one direction, and then in the other direction and a Poincare plot generated for each direction, the two surfaces overlap with the result shown in Figure 4 (a). The field lines all lie on the same surface, which is known as a manifold. When this procedure is repeated with the RMP coils applied, the two manifolds differ as a result of the 3D nature of the field, giving rise to structures at the X point as shown in Figure 4 (b) (Wingen *et al.* (2009)). The tangled field in the X point region leads to the formation of lobes.

The lobes generated by the RMP field can be modelled using the vacuum modelling code ERGOS (Nardon *et al.* (2007)). The vacuum modelling code takes the background magnetic field from the plasma and adds the field from the RMP coils, assuming that there is no plasma response. Figure 5 shows a Poincare plot of a poloidal cross section through the plasma with the RMP coils off with the unperturbed LCFS and X point shown. The colour indicates the minimum depth to which the field line penetrates into the plasma in terms of normalised flux

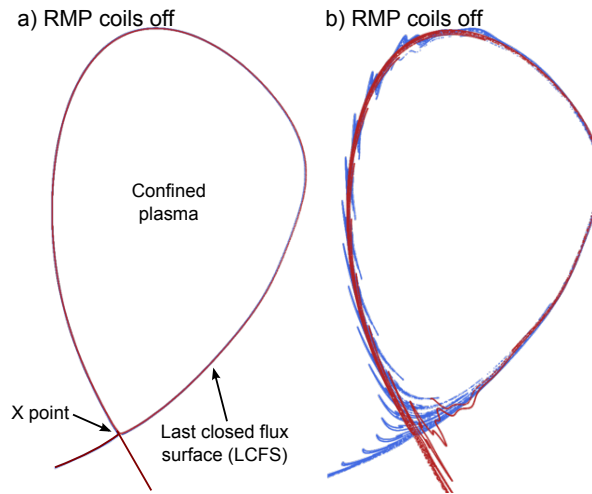


Figure 4. The stable and unstable manifolds in the plasma for the case of (a) no RMP field applied and (b) RMP field applied. The application of the RMP field gives rise to the formation of the lobes as a result of the intersection of the stable and unstable manifolds.

(Ψ_N), where $\Psi_N = 0$ is defined to be the axis of the plasma and $\Psi_N = 1$ at the LCFS. The nested flux surfaces expected in a confined plasma can be seen. In Figure 6 the Poincare plot is repeated with the coils on using a toroidal mode number of $n=6$ and 5.6 kAT in each coil. The modelled image clearly shows the formation of the lobes and the depth to which the field lines in the lobes penetrate into the plasma. The toroidal mode number of the applied perturbation determines the number of lobes present, with higher toroidal mode numbers of the applied RMP field giving rise to more lobes.

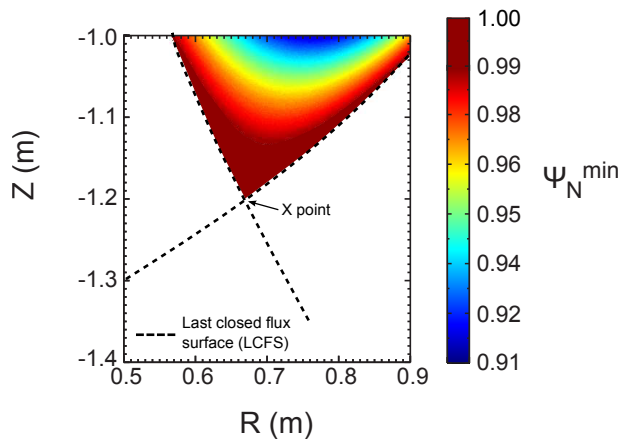


Figure 5. Output of field line tracing without the RMP coils applied. The colour indicates the depth into the plasma (in terms of normalised flux) to which the field line penetrates. The nested set of flux surface expected in a confined tokamak plasma can be seen.

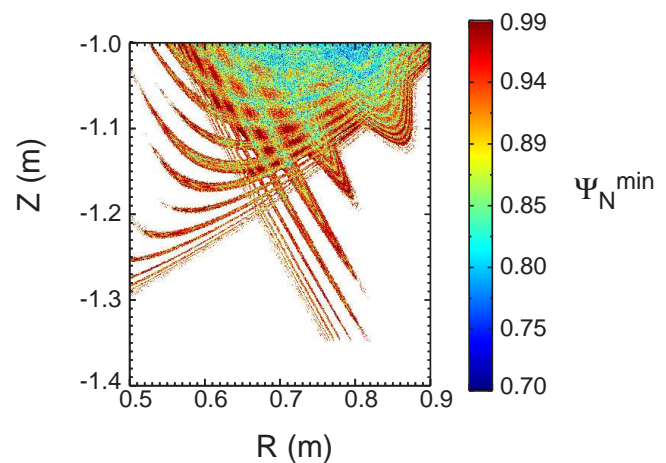


Figure 6. Field line tracing with the RMP coils applied and no screening of the RMP field from the plasma. The colour indicates the depth into the plasma to which the field line penetrates. The lobe structures can be clearly seen.

The lobe structures predicted by the modelling in Figure 6 have recently been observed on MAST via high speed imaging of the X point region (Kirk *et al.* (2012a)). The He II filtering has been used to image the plasma as emission at this wavelength is localised to the plasma edge. The imaging has a spatial resolution of 1.8 mm and a frame rate of 500 Hz during the period where the coils are applied. The imaging of the X point region is shown in Figure 7, with panel (a) showing the plasma prior to the coils being applied and panel (b) with the coils applied. The lobes can clearly be seen in the coils on image and the formation of the lobes is simultaneous with the increase in ELM frequency, confirming that the lobes and the effect of the RMP coils on the ELM frequency are associated with each other.

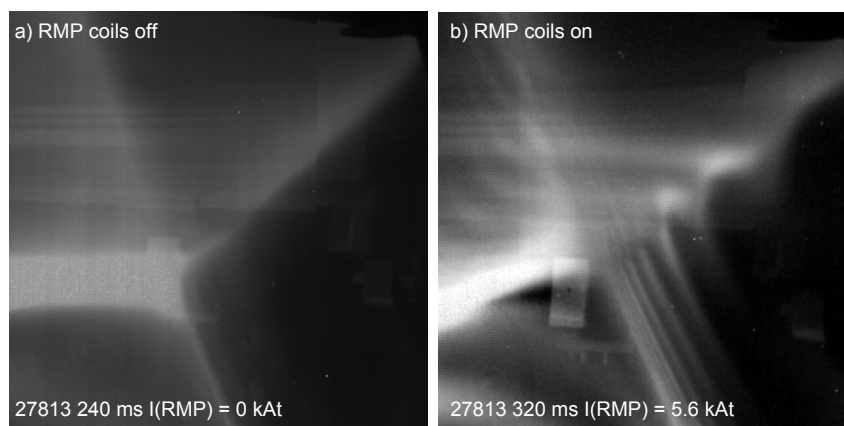


Figure 7. Filtered camera images (He II) showing the emission from the plasma edge in the case of (a) discharge with the RMP coils off and in (b) the coils on. The formation of the lobes between the coils on and the coils off case can clearly be seen. The applied RMP field has a toroidal mode, $n=6$, and a current of 5.6kAt.

The imaging of the lobes can be compared with modelling of the lobes (Kirk *et al.* (2012b)) using the vacuum field line tracing code. The intensity of the helium emission as a function of Ψ_N can be measured experimentally in the coils off case, this information can then be used to determine the intensity of the emission for an RMP applied case by using the result of the vacuum field line tracing shown in Figure 6 and forward modelling the emission expected for the lobes. The result of this modelling for the vacuum field line tracing result (Figure 6) is shown in Figure 8 (a) and can be compared with the image shown in Figure 7 (b). It is clear from comparing these figures that the modelling accurately reproduces the structure and location of the lobes expected when the coils are applied. However, the extent of the lobes as measured from the LCFS to the end of the lobe differs between the modelled and measured images. Simulation and experiment have shown that the lobe length is set by the size of the applied RMP field, with higher fields generating larger lobes (Cahyna *et al.* (2011)). As the modelled lobes are longer than those measured, this would suggest that the applied RMP field is being reduced by some mechanism. The vacuum modelling of the plasma neglects the effect of the plasma response to the applied external field, which acts to cancel out the applied field of the coils (Bécoulet *et al.* (2012)), thereby explaining the differences seen between the modelled images and the experimental measurements.

4. Plasma response to RMP fields

The screening of the applied field by the plasma is performed by currents induced inside the plasma. The induced currents on field lines which close on themselves after a finite number of poloidal turns (rational surfaces) oppose the formation of magnetic islands. One method to

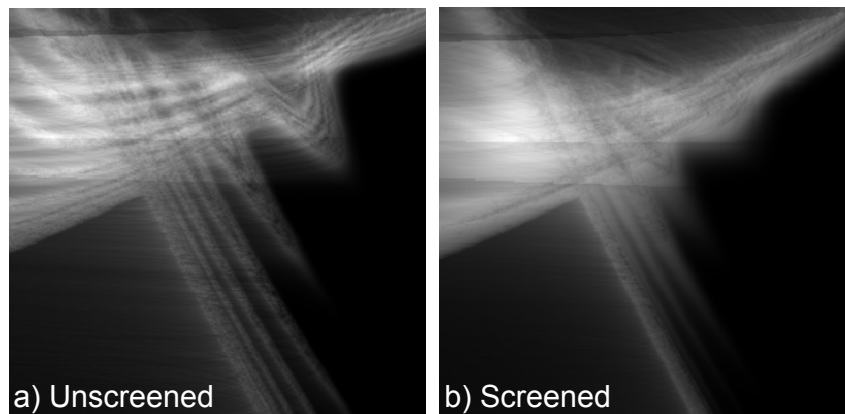


Figure 8. Modelling of the He II emission from the plasma based on the depth to which a field line penetrates into the plasma. The simulated image in panel (a) is for a coil current of 5.6kAt in an $n=6$ configuration without any screening of the RMP field from the plasma response taken into account. Panel (b) shows the same modelling repeated using an ad-hoc method to determine the screening of the RMP field by the plasma.

model the screening is to use an ad-hoc approach (Cahyna *et al.* (2011)). In this approach the screening response of the plasma is found by determining the RMP field at each of the rational surfaces and calculating the current required, on a given rational, surface to cancel out the field. The number of surfaces, and hence the radius of the plasma inside which the screening occurs, can be adjusted to best match the experimentally measured lobe size. Figure 9 is a Poincare plot showing the poloidal cross section of an unscreened plasma. The island chains are formed at the rational surfaces, with the largest islands present on the surface at $\Psi_N = 0.77$ which corresponds to a field line with a poloidal mode number of $m=7$. The screening effect is shown in Figure 10 where the current applied to the rational surface has cancelled out the islands, leading to the formation of a set of nested flux surfaces as seen in plasmas without the coils applied. The screening in Figure 10 acts over the surfaces $7 \leq m \leq 18$ with the shaded region in the figure showing the region of plasma which is unscreened.

The screened field can be used to generate a simulated image of the lobe structures as was performed for the unscreened field. The modelled image with screening applied is shown in Figure 8 (b). Comparison of Figure 8 (b) and the measured image (Figure 7 (b)) now show good agreement with the length of the lobes. The good match in the lobe length suggests that the RMP field is screened over 98% of the plasma radius, with penetration of the applied field across only 2-4% of the outer region of the plasma. Despite the low penetration of the applied field into the plasma, mitigation of the ELMs has been observed along with the formation of the lobe structures at the onset of the mitigation effect.

5. Conclusion

In a tokamak, the sudden ejection of a filament of plasma as a result of exceeding a critical pressure limit is known as an edge localised mode (ELM). These ELM events produce heat and particle fluxes to the divertor surfaces in the tokamak due to the energy contained within the filament of plasma. ELMs have the potential to limit the lifetime of the ITER divertor, and so a means of ELM control is required. One scheme of ELM control is the application of a non-axisymmetric field to perturb the plasma edge. This form of ELM control been seen to be manifest as ELM mitigation, (where the ELM frequency is increased which decreases the size of each ELM) or as ELM suppression, where the ELMs are removed completely. ELM mitigation

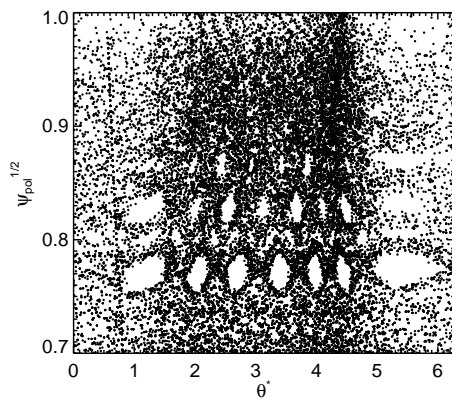


Figure 9. Poincare plot of the flux surface in a plasma with RMP coils applied at full current without any screening from the plasma response. The applied field leads to the formation of magnetic islands at the rational flux surfaces.

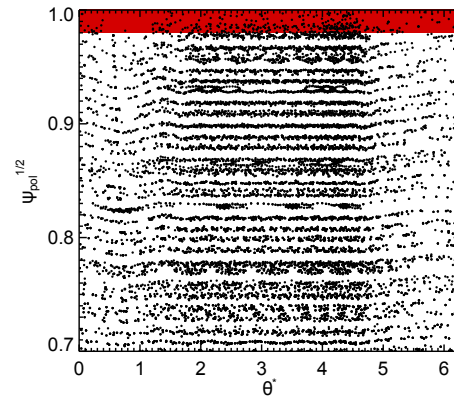


Figure 10. Poincare plot of the flux surfaces in the plasma with the RMP coils applied and a screening response from the plasma. The shaded region indicates where there is no screening and the RMP field penetrates the plasma.

has been achieved in MAST, with a five fold increase in the ELM frequency and corresponding decrease in the energy loss per ELM when a RMP field is applied. The applied RMP field produces a 3D magnetic field which gives rise to tangles in the magnetic field at the X point of the plasma. Imaging of the X point region of the plasma has confirmed that the tangled magnetic field produces lobes which form at the onset of the ELM mitigation. The plasma acts to screen the penetration of the RMP field from the plasma, thereby decreasing the amplitude of the RMP field experienced by the plasma. Modelling of the lobe structures including this screening has shown that the RMP field only needs to penetrate the outer 2-4% of the plasma radius to give rise to an effect on the ELMs. It is clear from the comparison of the vacuum modelling and the experimental data that there is significant screening of the applied perturbation as a result of the plasma response. The plasma response acts to reduce the region over which the magnetic islands are formed. The effect on the stability can also be understood by the formation of the lobes. The lobes act to perturb the plasma boundary and it has been suggested Chapman *et al.* (2012) that this acts to reduce the pressure gradient required for the onset of the ELMs. The reduction of the pressure gradient required by the lobes matches the experimental observations of ELM mitigation whereby the RMP coils act to increase the ELM frequency and decrease the ELM size. It should be noted that the modelling underlying the work on the effect of lobe stability is ideal, and a full treatment using resistive analysis is required which is the subject of future analysis.

Acknowledgments

This work was part funded by the RCUK Energy Programme under grant EP/I501045 and the European Communities under the Contract of Association between EURATOM and CCFE. The views and opinions expressed herein do not necessarily reflect those of the European Commission.

References

BÉCOULET, M. *et al.* 2012 Screening of resonant magnetic perturbations by flows in tokamaks. *Nucl. Fusion* **52**, 054003.

- CAHYNA, P. *et al.* 2011 Model for screening of resonant magnetic perturbations by plasma in a realistic tokamak geometry and its impact on divertor strike points. *J. Nucl. Mater.* **415**, S927–31.
- CHAPMAN, I. *et al.* 2012 Towards understanding ELM mitigation: the effect of axisymmetric lobe structures near the X-point on ELM stability **52**, 123006.
- EVANS, T. *et al.* 2004 Suppression of large edge-localized modes in high-confinement DIII-D plasmas with a stochastic magnetic boundary. *Phys. Rev. Lett.* **92**, 235003.
- EVANS, T. *et al.* 2005 Experimental signatures of homoclinic tangles in poloidally diverted tokamaks. *J. Phys: Conf. Ser.* **7**, 174–90.
- FEDERICI, G. *et al.* 2003 Assessment of erosion of the ITER divertor targets during type I ELMS. *Plasma Phys. Control. Fusion* **45**, 1523–47.
- KIRK, A. *et al.* 2004 ELM characteristics in MAST. *Plasma Phys. Control. Fusion* **46**, 551–72.
- KIRK, A. *et al.* 2012a Observation of lobes near the X point in resonant magnetic perturbation experiments on MAST. *Phys. Rev. Lett.* **108**, 255003.
- KIRK, A. *et al.* 2012b Understanding ELM mitigation by resonant magnetic perturbations on MAST. Submitted to Nucl. Fusion.
- KIRK, A. *et al.* 2013 Effect of resonant magnetic perturbations with toroidal mode numbers of 4 and 6 on edge-localized modes in single null h-mode plasmas in mast. *Plasma Phys. Control. Fusion* **55**, 015006.
- LOARTE, A. *et al.* 2007 Chapter 4: Power and particle control. *Nucl. Fusion* **47**, S203–63.
- NARDON, E. *et al.* 2007 Edge localized modes control by resonant magnetic perturbations. *J. Nucl. Mater.* **363-365**, 1071.
- WAGNER, F. *et al.* 1982 Regime of improved confinement and high beta in neutral-beam-heated divertor discharges of the ASDEX tokamak. *Phys. Rev. Lett.* **49** (19), 1408–12.
- WINGEN, A. *et al.* 2009 High resolution numerical studies of separatrix splitting due to non-axisymmetric perturbation in DIII-D. *Nucl. Fusion* **49**, 055027.
- ZOHM, H. 1996 Edge localised modes (ELMs). *Plasma Phys. and Control. Fusion* **38**, 105–28.